ADVANCING EARTH AND SPACE SCIENCES

Geophysical Research Letters

RESEARCH LETTER
10.1029/2022GL102101

Future Response of Antarctic Continental Shelf Temperatures to Ice Shelf Basal Melting and Calving

Max Thomas[1], Jeff K. Ridley[2], Inga J. Smith[1], David P. Stevens[3], Paul R. Holland[4], and Shona Mackie[1]

[1]Department of Physics, University of Otago, Dunedin, New Zealand, [2]Met Office, Exeter, UK, [3]Centre for Ocean and Atmospheric Sciences, School of Mathematics, University of East Anglia, Norwich, UK, [4]British Antarctic Survey, Cambridge, UK

Key Points:

- A glacial melt projection is added to a 1° coupled climate model under SSP5-8.5 to investigate ocean temperature feedbacks
- Additional glacial melt cools the Eastern Ross, Amundsen, and Bellingshausen seas at depth, but warms elsewhere
- The addition of glacial melt at depth is necessary to generate the cooling response

Supporting Information:

Supporting Information may be found in the online version of this article.

Correspondence to:

M. Thomas,
max.thomas@otago.ac.nz

Citation:

Thomas, M., Ridley, J. K., Smith, I. J., Stevens, D. P., Holland, P. R., & Mackie, S. (2023). Future response of Antarctic continental shelf temperatures to ice shelf basal melting and calving. *Geophysical Research Letters*, *50*, e2022GL102101. https://doi.org/10.1029/2022GL102101

Received 18 NOV 2022
Accepted 23 AUG 2023

Author Contributions:

Conceptualization: Max Thomas, Jeff K. Ridley, Inga J. Smith, David P. Stevens, Paul R. Holland, Shona Mackie
Data curation: Max Thomas
Funding acquisition: Inga J. Smith
Investigation: Max Thomas
Methodology: Jeff K. Ridley, David P. Stevens
Software: Jeff K. Ridley
Supervision: Inga J. Smith
Visualization: Max Thomas
Writing – original draft: Max Thomas
Writing – review & editing: Jeff K. Ridley, Inga J. Smith, Paul R. Holland, Shona Mackie

Abstract We investigate feedbacks between subsurface continental shelf ocean temperatures and Antarctic glacial melt using a coupled climate model. The model was forced with SSP5-8.5 and an uncoupled projection of basal melt and calving fluxes. SSP5-8.5 forcing with fixed pre-industrial glacial melt warms all continental shelves, such that historically "cool" and "fresh" shelves transition to "warm." Additional glacial melt, added at depth, cools the Eastern Ross, Amundsen, and Bellingshausen seas, suggesting a negative feedback on basal melt—a novel result for a coarse resolution coupled model. From the Weddell Sea, along East Antarctica, and into the western Ross Sea—where continental shelves transition to a "warm" state—additional glacial melt increases temperatures at the continental shelf sea floor, suggesting a positive feedback. The sign of the glacial melt–subsurface temperature feedback is critically dependent on continental shelf properties, climate state, and the vertical distribution of glacial melt inputs.

Plain Language Summary Antarctic ice shelves lose mass as freshwater—primarily from melting at their base and when icebergs break off. We know that the rate at which Antarctic ice shelves are losing mass is increasing and we expect this freshwater input into the ocean to increase further in a warmer world. Most climate models do not include a representation of this changing freshwater input, and its climatic impacts are uncertain. One particularly important climate impact is how the additional freshwater changes the subsurface ocean temperature. If freshwater warms/cools the coastal ocean it could increase/decrease melt in a positive/negative feedback loop. But existing studies disagree about this effect and even about the sign of the feedback. We added a timeseries of freshwater input to a climate model and ran experiments with strong climate warming to investigate this feedback. The sign of the feedback varies by region. Where climate change drives a cold coastal ocean to transition to a new warmer state, we find that freshwater causes a strong additional warming (a positive feedback). Where the coastal ocean is already warm in the present day and warms in future, freshwater reduces this warming (a negative feedback). To achieve the negative feedback freshwater must be added at depth.

1. Introduction

Observations show that Antarctica is losing mass as freshwater at an increasing rate (Rignot et al., 2019; Shepherd et al., 2019). Antarctic ice shelf basal melt and iceberg calving are projected to increase in a warming climate (DeConto & Pollard, 2016; Golledge et al., 2019; Seroussi et al., 2020), affecting surface temperature and precipitation (Bronselaer et al., 2018), sea-ice area (Bintanja et al., 2013), and bottom water production (Li et al., 2023; Mackie et al., 2020a; Pauling et al., 2016, 2017) and feeding back on ocean temperatures and basal melt (Bronselaer et al., 2018; Golledge et al., 2019). Fully coupled ice sheet/shelf–ocean–atmosphere modeling is in its infancy (Pelletier et al., 2022; Siahaan et al., 2022; Smith et al., 2021) and changing basal melt and calving are not represented in CMIP6 coupled climate models. Crucial uncertainties follow from this omission. For example, there is disagreement about the sign of the feedback between Antarctic freshwater input and basal melt (Beadling et al., 2022; Bronselaer et al., 2018; Moorman et al., 2020). This feedback is critically important to future climate because ice shelves restrict sea level rise by buttressing the Antarctic Ice Sheet (Rignot et al., 2004).

Most model studies find surface cooling and subsurface warming in response to increased Antarctic freshwater input at the surface (e.g., Bronselaer et al., 2018; Bintanja et al., 2013; Richardson et al., 2005; Stouffer et al., 2007; Swingedouw et al., 2008; Ma & Wu, 2011, with ocean horizontal resolution ranging from 1° to 3°) as increased stratification traps heat at depth. These results suggest a positive feedback, where ice-shelf melt leads to warming of the continental shelf at depth, driving further basal melt. By contrast, subsurface cooling has been modeled in the Amundsen and Bellingshausen seas (Beadling et al., 2022; Moorman et al., 2020)—and in the eastern Bellingshausen Sea (Li et al., 2023)—as a surface freshening induced strengthening of the Antarctic Slope Front and Antarctic Slope Current isolates the shelves from warm Circumpolar Deep Water (CDW) offshore. These results suggest a negative feedback that may reduce the rate of basal melt in West Antarctica. These cooling responses were found in relatively fine resolution models ($\frac{1}{4}^{\circ}$ to $\frac{1}{10}^{\circ}$), suggesting that such high resolution helps to simulate the strong Antarctic Slope Front (ASF) and Coastal Current (ACoC) that drives the cooling (Lockwood et al., 2021).

Here, we investigate the potential for regionally mixed-sign subsurface temperature changes induced by glacial melt in a coupled climate model with a 1° ocean resolution. We show that such mixed-sign temperature changes can occur under strong climate warming, providing glacial melt is added at depth.

2. Methods

All simulations were run using the coupled climate model HadGEM3-GC3.1-LL (Kuhlbrodt et al., 2018, and described in detail in Text S1 in Supporting Information S1). A constant flux of basal melt and calved icebergs are added at the southern boundary of the model's ocean, laterally distributed following Rignot et al. (2013, Figure S1 in Supporting Information S1). Basal melt is distributed vertically across the ice-shelf drafts as a latent heat conserving freshwater volume flux (Mathiot et al., 2017, their Figure 1d). There are no ice-shelf cavities. Calved icebergs undergo Lagrangian advection based on ocean currents (Marsh et al., 2015) and iceberg melt is deposited as a latent heat conserving volume flux to the top ocean grid cell. The total basal melt and calving flux is set to a steady value of 1,771 Gt.a^{-1} in the configuration for all HadGEM3-GC3.1-LL CMIP6 submissions, and was tuned to keep the pre-industrial ocean in salinity balance (Williams et al., 2018). Increases in surface melt over Antarctica are re-routed to the Southern Ocean as liquid runoff.

For our experiment (which we call SSP585FW), we ran a four member ensemble of HadGEM3-GC3.1-LL under SSP5-8.5 forcing (O'Neill et al., 2017) and included a representation of changing Antarctic basal melt and calving as a freshwater flux (see Table S1 in Supporting Information S1 for an experiment list). The additional freshwater flux was derived from the Ice Sheet Model Intercomparison for CMIP6 (ISMIP6) projections of basal melt (Seroussi et al., 2020). We chose data derived from RCP8.5 forcing; a "core" climate model (NorESM1, Barthel et al., 2020); and for which RCP2.6 data were also available. More precisely, we used Experiment 5. ISMIP6 present only spatially integrated basal melt rates, so we scaled the projected basal melt by present day observations of the basal melt to calving flux ratio (Rignot et al., 2013, 55% basal melt to 45% calving) to get a total Antarctic basal melt plus calving flux. We impose this total extra glacial melt timeseries as a polynomial (Figure 1). This extra glacial melt was added to the pre-industrial basal melt plus calving flux, scaled by the Rignot et al. (2013) spatial distribution, and results in approximately 5,500 Gt/a extra glacial melt in 2100 relative to 2015.

Our ensemble members branch in 2015 from the same historical simulations as the model's CMIP6 SSP5-8.5 submissions (which we use as a control, and call SSP585). Antarctica also loses freshwater as runoff, which does not change basal melt and calving fluxes. The sum of Antarctic runoff is similar in SSP585 and SSP585FW (Figure 1), so the ISMIP6 derived glacial melt perturbation dominates the freshwater signal in our experiment. We also present data from Historical HadGEM3-GC3.1-LL simulations—five member ensemble submitted to CMIP6—which we call HIST. In Section 3, we present ensemble mean data from SSP585FW averaged over 2080 to 2100, where the additional glacial melt forcing is largest and the climate has experienced the full SSP5-8.5 warming. We use SSP585, averaged over the same period, as a control to isolate impacts from increased basal melt and calving. To isolate SSP5-8.5 impacts, we use the 1995 to 2015 average of HIST as a second control.

3. Results

3.1. Changes in 400 m Potential Temperature

We first describe temperature changes at 400 m depth (Figure 2), which highlight the regional variance in our results (Bronselaer et al., 2018; Golledge et al., 2019). Our version of the model does not include ice-shelf

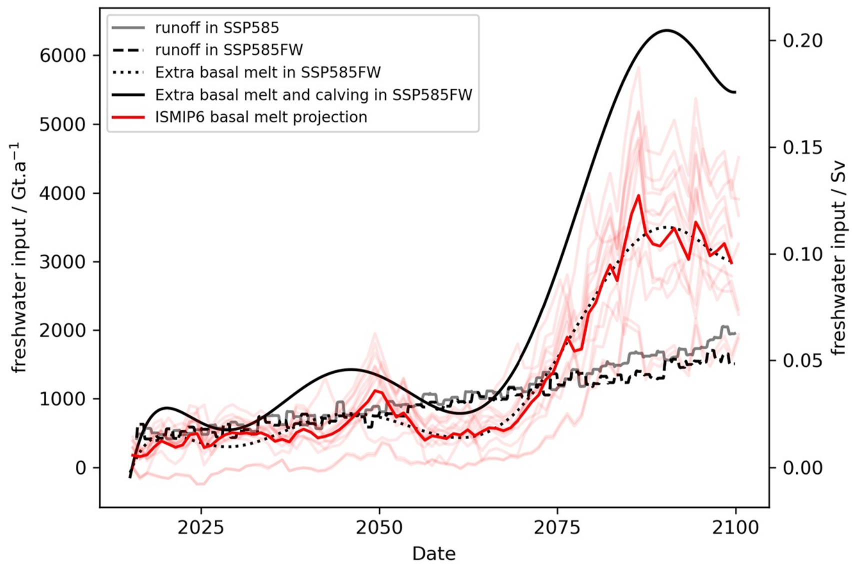

Figure 1. Timeseries of Antarctic glacial melt fluxes to the model's Southern Ocean. The dotted black line is the sum of Antarctic basal melt in HadGEM3-GC3.1-LL. The solid black line is the total basal melt plus calving flux for Antarctica, which was used to force HadGEM3-GC3.1-LL. The sum of the runoff from Antarctica is shown for the ensemble mean of the standard SSP5-8.5 runs (gray) and the runs where extra basal melt and calving were added (dashed black). For comparison, pale red lines are individual projections for Antarctic basal melt from ISMIP6 and the dark red line gives the multi-model mean. 1 Sv = 10^6 m^3 s^{-1}.

cavities, so we focus on temperature changes near the southern boundary of the model's ocean as changes in the temperature of these waters imply changes to basal melting of ice shelves (Bronselaer et al., 2018). In HIST (Figure 2a), the Amundsen and Bellingshausen continental shelves are flooded with warm (>0°C) water at 400 m, while the Weddell, East Antarctic, and Ross seas have near-freezing water on shelf. Strong warming over much of the Southern Ocean occurs in SSP585 by the end of the century, with much of the near-freezing water lost (Figures 2b and 2d). Strong warming also occurs in SSP585FW relative to HIST (Figures 2c and 2e). Relative to SSP585, SSP585FW has lost much more of the near-freezing water, and 400 m temperature is increased on the Weddell, East Antarctic, and Ross Sea shelves (Figure 2f). By contrast, there is a cooling in the Amundsen, Bellingshausen, and Eastern Ross Seas near the southern boundary of the model's ocean. This regional variation in the sign of the 400 m temperature change suggests that increased glacial melt may slow basal melt in the Amundsen and Bellingshausen Seas (negative feedback) but accelerate basal melt elsewhere (positive feedback).

3.2. Mechanisms Causing Temperature Changes

We investigate the cause of the regionally varying subsurface temperature response using sections from three example shelves, chosen to cover the range of continental shelf regimes in the model's Historical simulations (Figure 3). Following Thompson et al. (2018) we choose the Thwaites (252°E) and Amery (71°E) ice shelves as examples of "warm" and "fresh" continental shelves; and we use the Western Ross (177°E) as an example "cool" shelf, following Moorman et al. (2020).

As additional support for our arguments, we calculate three metrics over the continental shelves (south of the 1,000 m isobath) for the Amundsen and Bellingshausen (210°E to 290°E), the Western Ross (170°E to 180°E), and the East Antarctic near the Amery (60°E to 120°E): the integrated sea-ice area (a_{si}), sea-ice mass change by thermodynamic growth and melt (Δm_{si}), and Ekman pumping velocity (w_{Ek}). Ekman pumping, critical in setting isopycnal tilt, is calculated from the meridional and zonal surface ocean stress, and positive values indicate wind driven upwelling in a region. Modeled w_{Ek} is generally positive in the Southern Ocean south of the Westerly wind jet, but transitions to negative on shelf where the Easterlies drive downwelling against the coast (Figure S3 in Supporting Information S1). The thermodynamic growth of sea ice ($\Delta m_{si} > 0$) increases shelf salinity due to parameterized brine rejection, while melting sea ice ($\Delta m_{si} < 0$) freshens the ocean. In HIST, Δm_{si} is positive on shelf, indicating overall sea-ice production (Figure S4 in Supporting Information S1). Sea-ice area helps interpret Δm_{si} and w_{Ek} (Figure S5 in Supporting Information S1) in the next section.

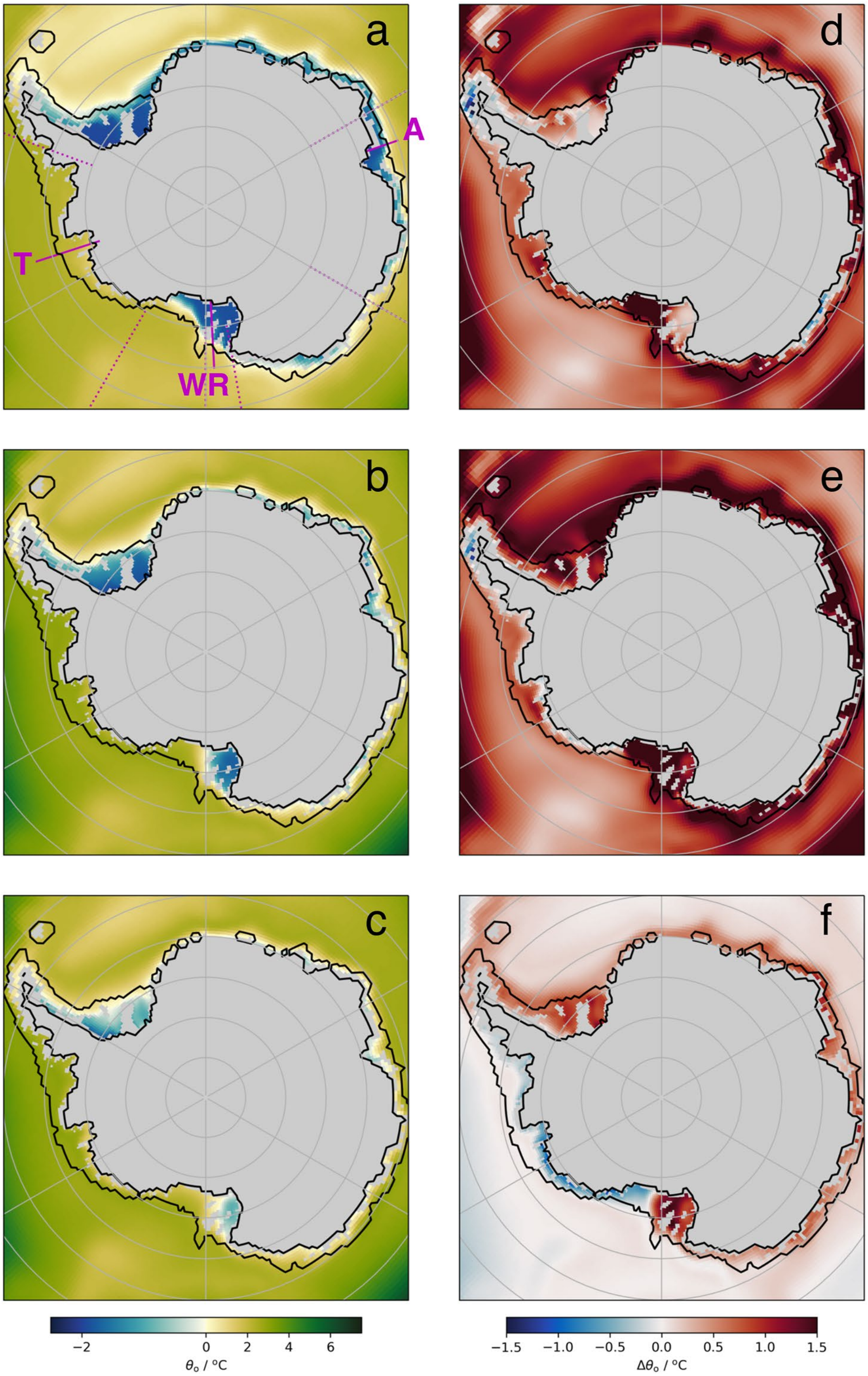

Figure 2. Potential temperature time mean at 400 m for (a) HIST, 1995 to 2015; (b) SSP585, 2080 to 2100; (c) SSP585FW, 2080 to 2100; (d) SSP5-8.5 induced change, (b) minus (a); (e) combined glacial melt and SSP5-8.5 induced change, (c) minus (a); and (f) glacial melt induced change, (c) minus (b). The 1,000 m isobath is shown by the black line; the locations of the sections in Figure 3 are shown by magenta lines in panel (a) (Thwaites, T; Western Ross, WR; Amery, A); and dotted magenta lines contain our chosen longitudes for the Amundsen and Bellingshausen (210°E to 290°E), the Western Ross (170°E to 180°E), and the East Antarctic near the Amery (60°E to 120°E).

10.1029/2022GL102101

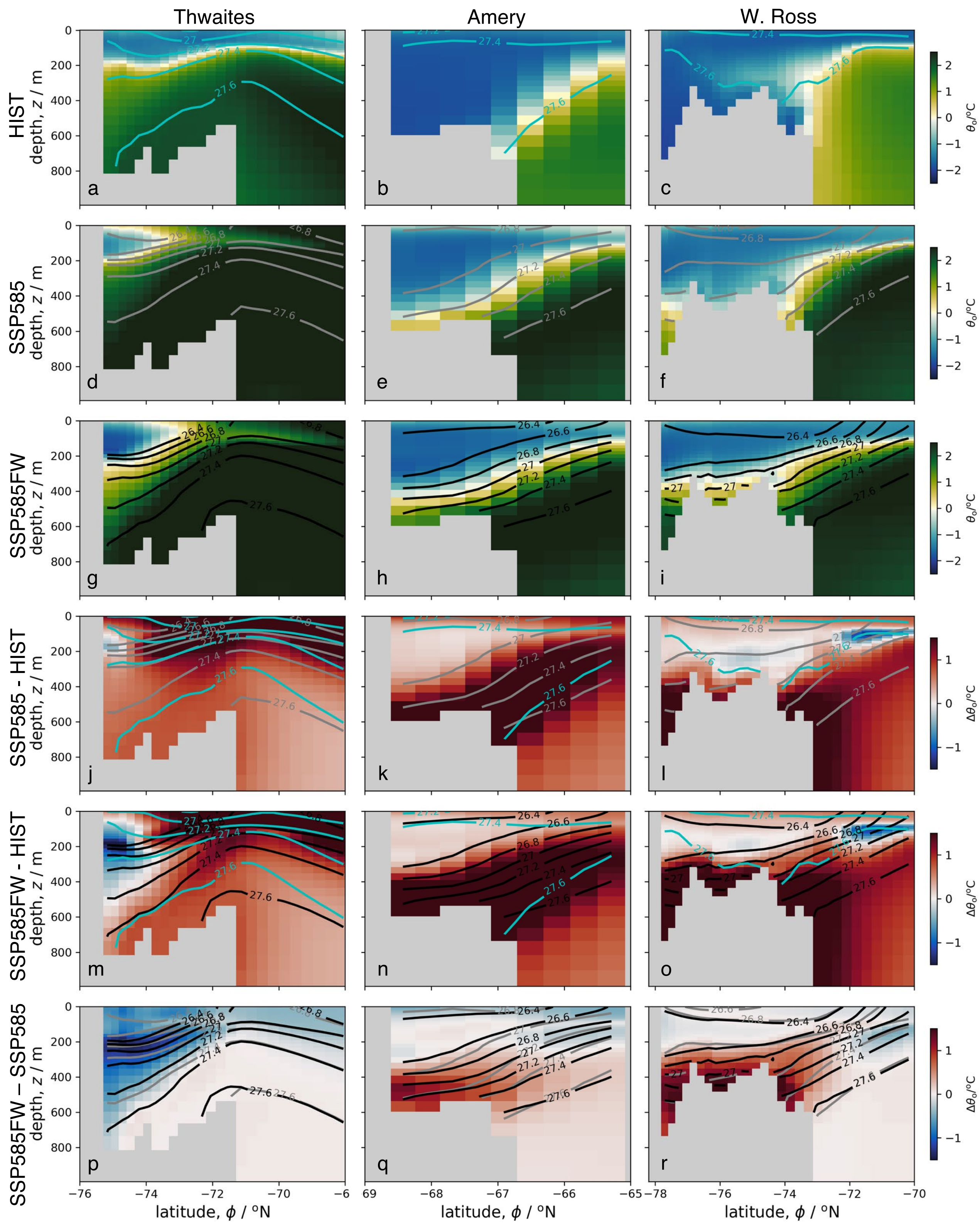

Figure 3. Potential temperature offshore of Thwaites (252°E, panel a down), Amery (71°E, panel b down), and the Western Ross (177°E, panel c down). Section positions are marked on Figure 2a. (a–i) 20 years time means for: (a–c) 1995 to 2015 of HIST; (d–f) 2080 to 2100 of SSP585; and (g–i) 2080 to 2100 time mean of SSP585FW. (j–r) Anomaly plots showing the effect of: (j–l) SSP5-8.5 forcing (panels d–f minus panels a–c); (m–o) SSP5-8.5 and glacial melt forcing combined (panels g–i minus a–c); and (p–r) glacial melt forcing (panels g–i minus d–f). Contours show σ_0 isopycnals, with HIST, SSP585, and SSP585FW in cyan, gray, and black, respectively.

3.2.1. Climate Change Induced Changes

We first turn to the effect of strong climate warming induced by the SSP5-8.5 scenario by examining SSP585 and HIST. Circumpolar, contraction and strengthening of the Westerlies (Figure S2 in Supporting Information S1) causes a reduction in the integrated coastal easterly wind stress over the continental shelf, tending to reduce downwelling near the coast under SSP5-8.5 forcing (Figure S3 in Supporting Information S1). Warming under SSP5-8.5 decreases net sea-ice production, but Δm_{si} remains positive (Figure S4 in Supporting Information S1). Sea-ice area decreases under SSP5-8.5 forcing but is increased by extra glacial melt (Figure S5 in Supporting Information S1).

Off Thwaites, there is an along-isopycnal connection between warm off-shelf water and the southern boundary of the model's ocean in HIST (Figure 3). A cold surface layer extends off the continental shelf and down to around 200 m. The cold surface layer contracts toward the coast in SSP585, coincident with collapsed sea-ice cover in the Amundsen and Bellingshausen. Winter sea-ice area between 210°E and 290°E has decreased from 0.59 Mkm^2 in HIST to 0.07 Mkm^2 in SSP585. Freshening is confined mostly to the surface, as expected from decreases in sea-ice production (Δm_{si} decreases by 87%) and increases in precipitation (Figure S6 in Supporting Information S1) and runoff (Figure 1), and the continental shelf remains connected with off-shelf water along isopycnals. Strong warming of surface and off-shelf water under climate change therefore increases temperatures on the continental shelf in SSP585. Furthermore, w_{Ek} is negative in HIST, implying downwelling on the shelf. In SSP585, integrated w_{Ek} changes sign, implying an overall upwelling and increased wind driven CDW intrusions to the continental shelf.

Near the Amery Ice Shelf, isopycnals intersect the bathymmetry in HIST, so there is no along-isopycnal connection between warm off-shelf water and the southern boundary of the model's ocean. The incropping isopycnals are maintained by negative Ekman velocities driven by coastal easterlies (Thompson et al., 2018, and see Figures S2 and S3 in Supporting Information S1). In SSP585 the isopycnals slump, allowing warm water to flow onto the continental shelf, causing strong warming at depth. This could be explained by a reduction in Ekman downwelling on the shelf, which is 64% weaker in SSP585 relative to HIST over 60°E to 120°E. Also, freshening increases stratification (Figure S7 in Supporting Information S1), which drives warming of the shelf in two ways. First, stronger stratification provides a greater barrier to vertical exchanges, and reduces the efficiency of Ekman pumping on the shelf. Second, stronger stratification may allow isopycnals at the shelf break to flatten as more energy input is required to maintain a given isopycnal slope. Additional evidence for this process is provided by Figure S8h in Supporting Information S1, where additional glacial melt under pre-industrial forcing causes isopycnals to flatten in this region despite there being little change in the wind stress (Mackie et al., 2020a). Under SSP5-8.5 forcing the Amery transitions from a fresh to a warm continental shelf regime.

In the Western Ross Sea, the continental shelf is "cool" in the Historical data following Moorman et al. (2020). Dense, cool water sits on-shelf, with a direct isopycnal connection to warmer off-shelf water (Figure 3). A wedge of warmer water intrudes onto the continental shelf at 250 m over the top of dense water, similar to present day observations Castagno et al. (2017). In SSP585 the continental shelf density decreases (Figure 3). At the end of the century, warm and saline, off-shelf water is denser than the cold and fresh, on-shelf waters and flows directly to the southern boundary of the model's ocean along the continental-shelf base. Similar behavior was found by Siahaan et al. (2022) under SSP5-8.5 forcing in a similar model set up with open ice-shelf cavities. Consequently, the shelf base warms and the warm wedge cools. Freshening in SSP585 from increased runoff and precipitation drives the density decrease in the Western Ross, with just 5% lower net sea-ice production in SSP585 relative to HIST.

3.2.2. Glacial Melt Induced Changes

The Amundsen and Bellingshausen shelves are cooler in SSP585FW than SSP585 (Figures 2 and 3). There is no regime change (Thwaites stays "warm") but several confluent factors result in a mean cooling of the continental shelf. First, winter sea-ice area is increased in SSP585FW (0.22 Mkm^2) relative to SSP585 (0.07 Mkm^2) and more cold brine is injected on shelf (Δm_{si} is 3.4 times larger in SSP585FW than SSP585). Second, basal melt is added at the southern boundary of the model's ocean, where the latent heat fluxes cool the continental shelf waters. Third, while w_{Ek} transitions to positive in SSP585FW (3.1×10^{-7} m s^{-1}), it is less positive than SSP585 (7.6×10^{-7} m s^{-1}). Finally, the strong freshening at depth in SSP585FW steepens the on-shelf isopycnals, reducing along-isopycnal transport of warm off-shelf water to the southern boundary of the model's ocean (Figure 3).

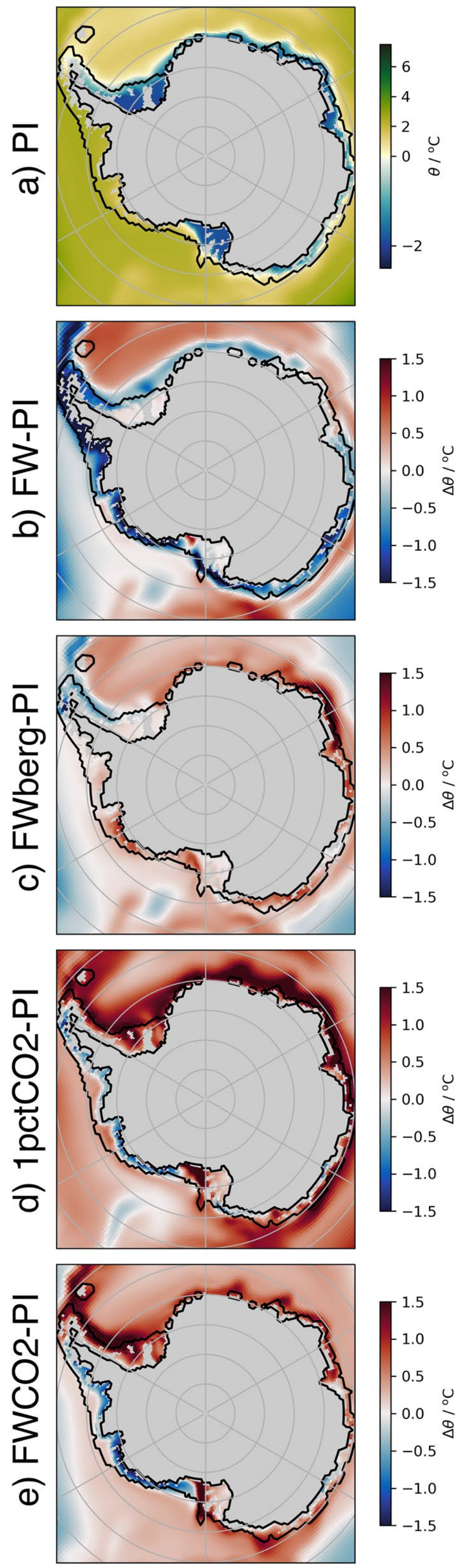

Figure 4. 80–100 years time means of 400 m potential temperature for (a) the pre-industrial CMIP6 submission for HadGEM3-GC3.1-LL (PI), and for four sensitivity experiments (see Mackie et al., 2020b, and as described in Section 4): (b) FW minus PI; (c) FWberg minus PI; (d) FWCO2 minus PI; and (e) FWCO2 minus 1pctCO2.

The cooling in this region found in previous, higher resolution, modeling studies (Beadling et al., 2022; Li et al., 2023; Moorman et al., 2020) was driven by strengthening of the Antarctic Slope Front combined with rerouting of cold waters from the Weddell Sea around the peninsula. Westward zonal ocean velocities do increase in SSP585 relative to HIST, and to a lesser extent in SSP585FW relative to SSP585 (Figure S9 in Supporting Information S1). However, the tendency in potential temperature from advection is more positive in SSP585FW relative to SSP585 (Figure S10 in Supporting Information S1), suggesting changes in advection partially offsets latent heat driven cooling rather than driving the cooling response.

In the Western Ross and Amery, there is a strong warming at the continental shelf bed in SSP585FW relative to SSP585 (Figure 3). The continental shelves are also fresher above around 500 m and saltier below (Figure S7 in Supporting Information S1). The base of the continental shelf is flooded with warm water in SSP585 and SSP585FW, which flows onto the continental shelf along flattened isopycnals (Section 3.2.1). The water column is more stratified in SSP585FW relative to SSP585, as evidenced by more and depressed isopycnals. This has two possible effects, as described above in Section 3.2.1. First, the increased stratification reduces vertical mixing of warmer, saltier deep waters over the continental shelf with colder, fresher surface waters, causing positive temperature and salinity anomalies at depth—similar to previous freshwater addition studies (e.g., Bronselaer et al., 2018; Pauling et al., 2016, 2017). Second, increased stratification may drive isopycnal flattening as a given tilt requires more energy to maintain, allowing more CDW onto the continental shelf. While latent heat extraction may cool deep continental shelf waters, the effect is overwhelmed by the change in water mass near the sea floor.

4. Discussion

Why do we see cooling at depth in some regions in response to additional glacial melt, when coarse resolution models generally report a circumpolar warming (e.g., Bintanja et al., 2013; Bronselaer et al., 2018; Ma & Wu, 2011; Richardson et al., 2005; Stouffer et al., 2007; Swingedouw et al., 2008)? Is the subsurface feedback robust to different climate scenarios? What can we learn about the response of a changing Southern Ocean to Antarctic glacial melt? We use experiments from Mackie et al. (2020a, 2020b) to help address these questions (Figure 4, Table S1 in Supporting Information S1). In those studies, HadGEM3-GC3.1-LL was run under various combinations of idealized forcing. Pre-industrial forcing was used in experiments FW and FWberg while 1% year-on-year increasing CO_2 was used in FWCO2 and 1pctCO2. In FW, FWberg, and FWCO2, an exponential increase in glacial melt was applied that resulted in 10 times more basal melt and calving after 100 years. The distribution of glacial melt inputs was the same as our SSP585FW runs in experiments labeled "FW," except for FWberg, where all glacial melt was added as icebergs.

The addition of freshwater at depth is a key reason for the subsurface cooling feedback in HadGEM3-GC3.1-LL. Under pre-industrial forcing, the effect of additional glacial melt due to both basal melt and calved icebergs is a circumpolar cooling (Figure 4b), while the effect of adding glacial melt exclusively at the surface (through iceberg melting) in FWberg is a circumpolar warming (Figure 4c). In FW, "warm" continental shelves cool from steepened isopycnals, increased sea ice, and latent heat fluxes (Figures S8 and S11 in Supporting Information S1), as in SSP585FW. "Cool" continental shelves transition to "fresh," and "fresh" shelves do not transition (though we do see some warming from isopycnal slumping), so both retain cold water. By contrast, isopycnals slump on "warm," "fresh," and "cool" continental shelves in FWberg sufficiently to route more CDW to the southern boundary of the model's ocean and warm at depth. Mathiot et al. (2017) showed that adding meltwater at depth (rather than just the surface) improved Southern Ocean properties in stand alone NEMO simulations, and that the parameterization we use where basal melt is distributed over the ice-shelf draft performs similarly well to explicitly open cavities. Observations near the Pine Island ice shelf show complex meltwater dynamics, with some meltwater remaining at depth (Naveira Garabato et al., 2017; Zheng et al., 2021). Adding basal melt at depth is therefore justified on model performance grounds and by physical considerations. Adding glacial melt across the ice shelf draft determines the sign of the subsurface temperature feedback under pre-industrial conditions.

Compared to these meltwater simulations with pre-industrial climate forcing (Mackie et al., 2020a, 2020b), the strong regional differences in the sign of the subsurface temperature response in SSP585FW therefore shows that the climate scenario must mediate the glacial melt–subsurface temperature feedback (Figure 2). We test this hypothesis by considering the effect of 1% CO_2 forcing on the sign of the feedback. Indeed, under 1% CO_2 forcing, the additional glacial melt input cools the ocean at 400 m relative to the pre-industrial control near the coast in the Amundsen and Bellingshausen seas, and warms continental shelves elsewhere (Figure 4d). Finally, we take the difference between FWCO2 and 1pctCO2 as this pair is directly comparable to our own experiments and control (SSP585FW and SSP585). The pattern in the glacial melt–subsurface temperature anomaly (Figure 4e) is very similar to our results (Figure 2f). Cooling of the Amundsen and Bellingshausen continental shelves is a robust response to increased glacial melt in our model. For the rest of Antarctica, where climate change pushes "cool" and "fresh" continental shelves to transition to "warm," glacial melt positively feeds back on subsurface temperature.

This regional pattern of subsurface warming and cooling is similar to that found by Moorman et al. (2020) (historical forcing, 0.1° horizontal resolution) and Beadling et al. (2022) (preindustrial forcing, 0.25° horizontal resolution) in experiments with surface freshwater added as a step function. Li et al. (2023), using essentially the same model as Moorman et al. (2020), find cooling in the eastern Bellingshausen Sea as freshwater is increased gradually under climate warming. These results can be explained by Antarctic Slope Front strengthening and rerouting of cold water from the Weddell Sea around the peninsula. In our lower resolution model, though we do see an acceleration in the ACoC, cooling along West Antarctica is driven by freshening at depth, which tilts isopycnals and cools by latent heat extraction. Improving model resolution changed the sign of the subsurface West Antarctic temperature response (Beadling et al., 2022; Li et al., 2023; Moorman et al., 2020) relative to coarse resolution freshening studies (e.g., Bronselaer et al., 2018). Two novelties of our study are that improving the depth distribution of freshwater inputs in a coarse resolution model also cools this region, and that the cooling effect was shown to persist under SSP5-8.5 forcing. As the climate modeling community moves toward inclusion of changing Antarctic basal melt in projections, care should be taken with regards to the depth distribution.

HadGEM3-GC3.1-LL performs well in the Southern Ocean among climate models with a 1° ocean resolution. The oceanographic structure off Thwaites ("warm") and Amery ("fresh") is consistent with Thompson et al. (2018). While HadGEM3-GC3.1-LL cannot produce the "V" shaped isopycnals characteristic of "dense" regimes, it does produce a "cool" (Moorman et al., 2020) Western Ross Sea, which is most similar to "dense." The Ross Gyre is reproduced well in UKESM1 (Gómez-Valdivia et al., 2023)—for which HadGEM3-GC3.1-LL is the physical core (Sellar et al., 2019)—and sea-ice area is captured within observational uncertainty (Roach et al., 2020). HadGEM3-GC3.1-LL is therefore a reasonable model to explore the freshening response. There are, however, major caveats to such coarse resolution, which hampers representation of the ASF, requires parameterized eddies and tides, and does not reproduce cascading dense overflows. These deficiencies influence heat transport across the shelf break (e.g., Purich & England, 2021) and too often lead to Antarctic Bottom Water formed by open ocean convection (Heuzé, 2021). HadGEM3-GC3.1-LL also has biases in dense shelf water formation, which may impact our conclusions for the Western Ross. HadGEM3-GC3.1-LL is too fresh in the Western Ross Sea relative to observations (Figure S12 in Supporting Information S1), which may accelerate the "cool" to "warm" state change. The proposed mechanism of increased stratification slumping isopycnals (Section 3.2.1) may be resolution dependent, given it was not found by Moorman et al. (2020) and Beadling et al. (2022), though similar behavior was noted by Li et al. (2023). Nevertheless, our results are important as Coupled Climate and Earth System Models with a 1° ocean resolution, despite their limitations, are likely to remain useful tools for future climate research. Furthermore, our results motivate higher resolution studies with glacial melt added at depth.

The ISMIP6 projected basal melt gives a plausible timeseries (intermediate between Golledge et al. (2019) and DeConto and Pollard (2016) RCP8.5 projections) that allows us to perform a controlled experiment. Large changes in Antarctic glacial melt are implied by ISMIP6 (more than double present day), while some climate model studies found significant climate impacts from freshwater forcing changes of a few percent (Bintanja et al., 2013). Interrogating the sensitivity of projections to plausible freshwater changes is therefore justified. A caveat to our approach is that the change in Antarctic basal melt and calving is uncoupled from modeled ocean and atmosphere temperatures. While we can diagnose likely feedbacks on basal melt via temperature changes at the southern boundary of the model's ocean (Bronselaer et al., 2018), the basal melt in our model does not respond. Furthermore, increases in glacial melt input are scaled by present day distributions (both laterally, and the ratio of basal melt to calving) which may not hold in future. Fully coupled climate–ice sheet models have only recently been developed (Pelletier et al., 2022; Smith et al., 2021). Our results show that feedbacks between basal melt and calving fluxes and continental-shelf ocean temperatures are complex, and may vary with climate state and by region.

5. Conclusions

The inclusion of time-varying Antarctic basal melt and calving fluxes feeds back strongly on continental-shelf temperature around Antarctica. Under SSP5-8.5 climate warming, additional glacial melt cools the subsurface in the Amundsen and Bellingshausen seas—a novel result in 1° ocean resolution modeling—and warms the subsurface from the western Ross Sea, across East Antarctica, and into the Weddell Sea. This regional heterogeneity is driven by the combined effects of SSP5-8.5 and glacial melt. With no climate change, additional glacial melt cools all Antarctic continental shelves. When those shelves transition under climate change, additional glacial melt accentuates warming over the continental shelf. The vertical distribution of glacial melt inputs strongly controls the subsurface temperature feedback. When freshwater is added exclusively at the surface, a circumpolar subsurface warming is generated. The inclusion of changing Antarctic basal melt and calving fluxes is a priority for the climate modeling community. The effect of these fluxes on modeled climate is complex, with the sign of the induced subsurface temperature feedback depending on both the vertical distribution of inputs and the climate state.

Data Availability Statement

Replication data are available at https://doi.org/10.5281/zenodo.8309934. Links to CMIP6 data, and data from Mackie et al. (2020a, 2020b), are given in Table S1 in Supporting Information S1. The ocean model code used to generate the majority of data used in this paper, is available from https://www.nemo-ocean.eu/doc/node4.html. Reproduction code is at https://github.com/MaxThomas90/Thomas-et-al-2023GRL.

Acknowledgments

MT and IJS were supported by the Deep South National Science Challenge (MBIE contract number C01X1412) and the Antarctic Science Platform (University of Otago subcontract 19424 from VUW's ASP Project 4 contract with Antarctica New Zealand through MBIE SSIF Programmes Investment contract number ANTA1801). The authors acknowledge use of New Zealand eScience Infrastructure (NeSI) high performance computing facilities, consulting support, and training services. New Zealand's national facilities are provided by NeSI and funded jointly by NeSI's collaborator institutions and through MBIE's Research Infrastructure programme. JR was supported by the Met Office Hadley Centre Climate Programme funded by DBEIS and Defra. Thanks to Jonny Williams (NIWA) for help setting up and working with the model. Open access publishing facilitated by University of Otago, as part of the Wiley - University of Otago agreement via the Council of Australian University Librarians.

References

Barthel, A., Agosta, C., Little, C. M., Hattermann, T., Jourdain, N. C., Goelzer, H., et al. (2020). CMIP5 model selection for ISMIP6 ice sheet model forcing: Greenland and Antarctica. *The Cryosphere*, *14*(3), 855–879. https://doi.org/10.5194/tc-14-855-2020

Beadling, R., Krasting, J., Griffies, S., Hurlin, W., Bronselaer, B., Russell, J., et al. (2022). Importance of the Antarctic Slope Current in the Southern Ocean response to ice sheet melt and wind stress change. *Journal of Geophysical Research: Oceans*, *127*(5), e2021JC017608. https://doi.org/10.1029/2021JC017608

Bintanja, R., van Oldenborgh, G. J., Drijfhout, S., Wouters, B., & Katsman, C. (2013). Important role for ocean warming and increased ice-shelf melt in Antarctic sea-ice expansion. *Nature Geoscience*, *6*(5), 376–379. https://doi.org/10.1038/ngeo1767

Bronselaer, B., Winton, M., Griffies, S. M., Hurlin, W. J., Rodgers, K. B., Sergienko, O. V., et al. (2018). Change in future climate due to Antarctic meltwater. *Nature*, *564*(7734), 53–58. https://doi.org/10.1038/s41586-018-0712-z

Castagno, P., Falco, P., Dinniman, M. S., Spezie, G., & Budillon, G. (2017). Temporal variability of the circumpolar deep water inflow onto the Ross Sea continental shelf. *Journal of Marine Systems*, *166*, 37–49. https://doi.org/10.1016/j.jmarsys.2016.05.006

DeConto, R. M., & Pollard, D. (2016). Contribution of Antarctica to past and future sea-level rise. *Nature*, *531*(7596), 591–597. https://doi.org/10.1038/nature17145

Golledge, N. R., Keller, E. D., Gomez, N., Naughten, K. A., Bernales, J., Trusel, L. D., & Edwards, T. L. (2019). Global environmental consequences of twenty-first-century ice-sheet melt. *Nature*, *566*(7742), 65–72. https://doi.org/10.1038/s41586-019-0889-9

Gómez-Valdivia, F., Holland, P. R., Siahaan, A., Dutrieux, P., & Young, E. (2023). Projected West Antarctic ocean warming caused by an expansion of the Ross Gyre. *Geophysical Research Letters*, *50*(6), e2023GL102978. https://doi.org/10.1029/2023GL102978

Heuzé, C. (2021). Antarctic bottom water and North Atlantic deep water in CMIP6 models. *Ocean Science*, *17*(1), 59–90. https://doi.org/10.5194/os-17-59-2021

Kuhlbrodt, T., Jones, C. G., Sellar, A., Storkey, D., Blockley, E., Stringer, M., et al. (2018). The low-resolution version of HadGEM3-gc3.1: Development and evaluation for global climate. *Journal of Advances in Modeling Earth Systems*, *10*(11), 2865–2888. https://doi.org/10.1029/2018MS001370

Li, Q., England, M. H., Hogg, A. M., Rintoul, S. R., & Morrison, A. K. (2023). Abyssal ocean overturning slowdown and warming driven by Antarctic meltwater. *Nature*, *615*(7954), 841–847. https://doi.org/10.1038/s41586-023-05762-w

Lockwood, J. W., Dufour, C. O., Griffies, S. M., & Winton, M. (2021). On the role of the Antarctic Slope Front on the occurrence of the Weddell Sea polynya under climate change. *Journal of Climate*, *34*(7), 2529–2548. https://doi.org/10.1175/JCLI-D-20-0069.1

Ma, H., & Wu, L. (2011). Global teleconnections in response to freshening over the Antarctic Ocean. *Journal of Climate*, *24*(4), 1071–1088. https://doi.org/10.1175/2010JCLI3634.1

Mackie, S., Smith, I. J., Ridley, J. K., Stevens, D. P., & Langhorne, P. J. (2020a). Climate response to increasing Antarctic iceberg and ice shelf melt. *Journal of Climate*, *33*(20), 8917–8938. https://doi.org/10.1175/JCLI-D-19-0881.1

Mackie, S., Smith, I. J., Ridley, J. K., Stevens, D. P., & Langhorne, P. J. (2020b). Interactions between increasing CO_2 and Antarctic melt rates. *Journal of Climate*, *33*(20), 8939–8956. https://doi.org/10.1175/JCLI-D-19-0882.1

Marsh, R., Ivchenko, V. O., Skliris, N., Alderson, S., Bigg, G. R., Madec, G., et al. (2015). NEMO–ICB (v1.0): Interactive icebergs in the NEMO ocean model globally configured at eddy-permitting resolution. *Geoscientific Model Development*, *8*(5), 1547–1562. https://doi.org/10.5194/gmd-8-1547-2015

Mathiot, P., Jenkins, A., Harris, C., & Madec, G. (2017). Explicit representation and parametrised impacts of under ice shelf seas in the z coordinate ocean model NEMO 3.6. *Geoscientific Model Development*, *10*(7), 2849–2874. https://doi.org/10.5194/gmd-10-2849-2017

Moorman, R., Morrison, A. K., & McC Hogg, A. (2020). Thermal responses to Antarctic ice shelf melt in an eddy-rich global ocean–sea ice model. *Journal of Climate*, *33*(15), 6599–6620. https://doi.org/10.1175/JCLI-D-19-0846.1

Naveira Garabato, A. C., Forryan, A., Dutrieux, P., Brannigan, L., Biddle, L. C., Heywood, K. J., et al. (2017). Vigorous lateral export of the meltwater outflow from beneath an Antarctic ice shelf. *Nature*, *542*(7640), 219–222. https://doi.org/10.1038/nature20825

O'Neill, B. C., Kriegler, E., Ebi, K. L., Kemp-Benedict, E., Riahi, K., Rothman, D. S., et al. (2017). The roads ahead: Narratives for shared socioeconomic pathways describing world futures in the 21st century. *Global Environmental Change*, *42*, 169–180. https://doi.org/10.1016/j.gloenvcha.2015.01.004

Pauling, A. G., Bitz, C. M., Smith, I. J., & Langhorne, P. J. (2016). The response of the Southern Ocean and Antarctic sea ice to freshwater from ice shelves in an Earth System Model. *Journal of Climate*, *29*(5), 1655–1672. https://doi.org/10.1175/JCLI-D-15-0501.1

Pauling, A. G., Smith, I. J., Langhorne, P. J., & Bitz, C. M. (2017). Time-dependent freshwater input from ice shelves: Impacts on Antarctic sea ice and the Southern Ocean in an Earth System Model. *Geophysical Research Letters*, *44*(20), 10–454. https://doi.org/10.1002/2017GL075017

Pelletier, C., Fichefet, T., Goosse, H., Haubner, K., Helsen, S., Huot, P.-V., et al. (2022). PARASO, a circum-Antarctic fully coupled ice-sheet–ocean–sea-ice–atmosphere–land model involving fETISh1.7, NEMO3.6, LIM3.6, COSMO5.0 and CLM4.5. *Geoscientific Model Development*, *15*(2), 553–594. https://doi.org/10.5194/gmd-15-553-2022

Purich, A., & England, M. H. (2021). Historical and future projected warming of Antarctic shelf bottom water in CMIP6 models. *Geophysical Research Letters*, *48*(10), e2021GL092752. https://doi.org/10.1029/2021GL092752

Richardson, G., Wadley, M. R., Heywood, K. J., Stevens, D. P., & Banks, H. T. (2005). Short-term climate response to a freshwater pulse in the Southern Ocean. *Geophysical Research Letters*, *32*(3), L03702. https://doi.org/10.1029/2004GL021586

Rignot, E., Casassa, G., Gogineni, P., Krabill, W., Rivera, A., & Thomas, R. (2004). Accelerated ice discharge from the Antarctic Peninsula following the collapse of Larsen B ice shelf. *Geophysical Research Letters*, *31*(18), L18401. https://doi.org/10.1029/2004GL020697

Rignot, E., Jacobs, S., Mouginot, J., & Scheuchl, B. (2013). Ice-shelf melting around Antarctica. *Science*, *341*(6143), 266–270. https://doi.org/10.1126/science.1235798

Rignot, E., Mouginot, J., Scheuchl, B., Van Den Broeke, M., Van Wessem, M. J., & Morlighem, M. (2019). Four decades of Antarctic ice sheet mass balance from 1979–2017. *Proceedings of the National Academy of Sciences*, *116*(4), 1095–1103. https://doi.org/10.1073/pnas.1812883116

Roach, L. A., Dörr, J., Holmes, C. R., Massonnet, F., Blockley, E. W., Notz, D., et al. (2020). Antarctic sea ice area in CMIP6. *Geophysical Research Letters*, *47*(9), e2019GL086729. https://doi.org/10.1029/2019GL086729

Sellar, A. A., Jones, C. G., Mulcahy, J. P., Tang, Y., Yool, A., Wiltshire, A., et al. (2019). UKESM1: Description and evaluation of the UK Earth System Model. *Journal of Advances in Modeling Earth Systems*, *11*(12), 4513–4558. https://doi.org/10.1029/2019MS001739

Seroussi, H., Nowicki, S., Payne, A. J., Goelzer, H., Lipscomb, W. H., Abe-Ouchi, A., et al. (2020). ISMIP6 Antarctica: A multi-model ensemble of the Antarctic ice sheet evolution over the 21st century. *The Cryosphere*, *14*(9), 3033–3070. https://doi.org/10.5194/tc-14-3033-2020

Shepherd, A., Gilbert, L., Muir, A. S., Konrad, H., McMillan, M., Slater, T., et al. (2019). Trends in Antarctic ice sheet elevation and mass. *Geophysical Research Letters*, *46*(14), 8174–8183. https://doi.org/10.1029/2019GL082182

Siahaan, A., Smith, R. S., Holland, P. R., Jenkins, A., Gregory, J. M., Lee, V., et al. (2022). The Antarctic contribution to 21st-century sea-level rise predicted by the UK Earth System Model with an interactive ice sheet. *The Cryosphere*, *16*(10), 4053–4086. https://doi.org/10.5194/tc-16-4053-2022

Smith, R. S., Mathiot, P., Siahaan, A., Lee, V., Cornford, S. L., Gregory, J. M., et al. (2021). Coupling the UK Earth System Model to dynamic models of the Greenland and Antarctic ice sheets. *Journal of Advances in Modeling Earth Systems*, *13*(10), e2021MS002520. https://doi.org/10.1029/2021MS002520

Stouffer, R. J., Seidov, D., & Haupt, B. J. (2007). Climate response to external sources of freshwater: North Atlantic versus the Southern Ocean. *Journal of Climate*, *20*(3), 436–448. https://doi.org/10.1175/JCLI4015.1

Swingedouw, D., Fichefet, T., Huybrechts, P., Goosse, H., Driesschaert, E., & Loutre, M.-F. (2008). Antarctic ice-sheet melting provides negative feedbacks on future climate warming. *Geophysical Research Letters*, *35*(17), L17705. https://doi.org/10.1029/2008GL034410

Thompson, A. F., Stewart, A. L., Spence, P., & Heywood, K. J. (2018). The Antarctic Slope current in a changing climate. *Reviews of Geophysics*, *56*(4), 741–770. https://doi.org/10.1029/2018RG000624

Williams, K., Copsey, D., Blockley, E., Bodas-Salcedo, A., Calvert, D., Comer, R., et al. (2018). The Met Office global coupled model 3.0 and 3.1 (GC3.0 and GC3.1) configurations. *Journal of Advances in Modeling Earth Systems*, *10*(2), 357–380. https://doi.org/10.1002/2017MS001115

Zheng, Y., Heywood, K. J., Webber, B. G., Stevens, D. P., Biddle, L. C., Boehme, L., & Loose, B. (2021). Winter seal-based observations reveal glacial meltwater surfacing in the southeastern Amundsen Sea. *Communications Earth & Environment*, *2*(1), 1–9. https://doi.org/10.1038/s43247-021-00111-z